Environmental and Molecular Mutagenesis 52:664–672 (2011)

Research Article

Induction of DNA Damage Signaling Genes in Benzidine-Treated HepG2 Cells

Ssu Ching Chen,[1]* You-Cheng Hseu,[2] Jia-Chuen Sung,[3] Chin-Hui Chen,[4,5] Lei-Chin Chen,[6] and King-Tom Chung[7]

[1]*Department of Life Science, National Central University, Chung-Li City, Taoyan Country, Taiwan, Republic of China*
[2]*Department of Cosmeceutics, China Medical University, Taichung, Taiwan*
[3]*Department of Biotechnology, National Kaohsiung Normal University, Kaohsiung, Taiwan, Republic of China*
[4]*School of Pharmacy, Taipei Medical University, Taipei, Taiwan, Republic of China*
[5]*Department of Medical Technology, Yuanpei Institute of Science and Technology, Hsin-Chu, Taiwan, Republic of China*
[6]*Department of Medical Nutrition, I-Shou University, Kaohsiung, Taiwan, Republic of China*
[7]*Department of Biology, The University of Memphis, Memphis, Tennessee*

We examined genotoxicity and DNA damage response in HepG2 cells following exposure to benzidine. Using the Comet assay, we showed that benzidine (50–200 μM) induces DNA damage in HepG2 cells. DNA damage signaling pathway-based PCR arrays were used to investigate expression changes in genes involved in cell-cycle arrest, apoptosis, and DNA repair and showed upregulation of 23 genes and downregulation of one gene in benzidine-treated cells. Induction of G2/M arrest and apoptosis was confirmed at the protein level. Real-time PCR and Western blots were used to demonstrate the expression of select DNA repair-associated genes from the PCR array. Upregulation of the p53 protein in benzidine-treated cells suggests the induction of the p53 DNA damage signaling pathway. Collectively, DNA damage response genes induced by benzidine indicate recruitment complex molecular machinery involved in DNA repair, cell-cycle arrest, and potentially, activation of the apoptosis. Environ. Mol. Mutagen. 52:664–672, 2011.

Key words: apoptosis; cell-cycle arrest; DNA repair; Comet assay

INTRODUCTION

Benzidine is used in the production of azo dyes that are used in the textile, paper, and leather industries [Chung et al., 1998]. The results of various studies have suggested that benzidine is mutagenic [Chung and Cerniglia, 1992]. For example, the mutagenicity of benzidine and its analogues has been shown using the *Salmonella* bacterial mutagenicity assay [Chung et al., 2000] and with the *Escherichia coli* DJ 702 *LacZ* reversion mutagenicity assay [Chen et al., 2006]. In addition, benzidine has been shown to act as a genotoxin in human lymphocytes using the Comet assay [Chen et al., 2003] and to induce sister chromatid exchange in rat and human hepatoma cells lines (HepG2) [Grady et al., 1986].

Benzidine is recognized as a human carcinogen [Makena and Chung, 2007a,b]. Numerous studies demonstrate that occupational exposure to benzidine causes bladder cancer in humans [Makena and Chung, 2007]. In addition to renal and transitional cell carcinomas in the bladder, benzidine may also act as a hepatocarcinogen [Morikawa et al., 1997]. Although it has been thoroughly studied, the mechanism underlying benzidine genotoxicity remains unclear.

Genotoxicity can be produced through the direct interaction of a compound or its metabolite and DNA. Alternatively, compounds that generate reactive oxygen species, induce cytotoxicity, or affect cell proliferation

*Correspondence to: S.C. Chen, Department of Life Sciences, National Central University, Chung-Li city, Taoyan, Taiwan, Republic of China. E-mail: osycchna@ksts.seed.net.tw

Received 8 February 2011; provisionally accepted 20 June 2011; and in final form 21 June 2011

DOI 10.1002/em.20669

Published online 4 August 2011 in Wiley Online Library (wileyonlinelibrary.com).

can negatively affect DNA integrity [Arbillaga et al., 2007]. The former categories of genotoxins are called DNA reactive, whereas the latter are called DNA nonreactive [Arbillaga et al., 2007]. Microarray technology can be used to discriminate between DNA reactive and DNA nonreactive genotoxins, because these different modes of action induce different gene expression profiles [Hu et al., 2004].

A DNA damage signaling pathway-based PCR array was used previously to investigate the expression of genes related to DNA damage and repair response in HepG2 cells treated with zidovudine [Wu et al., 2011]. Similarly, in the present study, we investigated expression changes in 84 genes associated with apoptosis, cell-cycle arrest, and DNA repair in HepG2 cells before and after benzidine treatment to obtain information on cellular mechanisms that operate in response to this compound. The aim of this study was to identify the biological pathways that are modulated by benzidine in vitro to elucidate its underlying genotoxic mechanisms.

MATERIALS AND METHODS

Materials

Benzidine, ammonium bicarbonate, dimethyl sulfoxide (DMSO), thiazolyl blue tetrazolium bromide (MTT), and 35% hydrogen peroxide were purchased from Sigma-Aldrich (Steinheim, Germany). Annexin V-FITC, propidium iodide (PI), and 10× binding buffer were purchased from BD Pharmingen (San Diego, USA). Fetal bovine serum and DMEM were purchased from Hyclone (LOGAN).

Cell Culture

HepG2 cells were grown in DMEM supplemented with 10% (v/v) fetal bovine serum, 2 mM L-glutamine, 50 U/ml penicillin, and 0.1 mg/ml streptomycin. Cells were grown in 25 cm^2 flasks at 37°C in a humidified atmosphere containing 5% CO_2. Fresh growth medium was added every 2 days until confluence was achieved.

Cell Treatment

Cells were cultured in six-well plates until 70% confluence was reached. Medium was then replaced with fresh serum-free medium containing 50–200 μM benzidine in DMSO. Negative controls were exposed to 0.5% DMSO, and the final concentration was used in benzidine-treated cultures. Cells were exposed for a total of 24 hr. Thereafter, cells were washed twice with Hank's buffered salt solution, harvested, and transferred to a-1.5 mL RNase-free centrifuge tube and spun at 300*g* for 5 min. An aliquot of each cell suspension was retained before centrifugation for use in the cytotoxicity and Comet assays. After centrifugation, the supernatant was removed, and total RNA was isolated for the pathway-specific real-time PCR array using Trizol (Invitrogen, Carlsbad, CA) according to the manufacturer's protocol (see below).

Cytotoxicity Assays

HepG2 cells were seeded onto 96-well plates at a density of 10^4 cells/well and incubated for 24 hr at 37°C. The medium was then replaced with fresh complete medium containing benzidine at the indicated doses and incubated for 24 hr. MTT (0.5 mg/ml) (Steinheim, Germany) was added to the medium, and then the plates were incubated for additional 3 hr. At the end of the MTT incubation, the medium was removed, and the formazon crystals were dissolved in DMSO. The optical density (OD) was measured at 570 nm (reference filter 690 nm) using a microplate spectroflurometer. Viability was determined by comparing the OD of the wells containing benzidine-treated cells with those of untreated cells. The results are expressed as the mean of at least three independent experiments.

Comet Assay

The Comet assay was performed under alkaline conditions using previously described methods [Wang et al., 2006; Wu et al., 2009]. At least 300 images were randomly selected from each sample and analyzed for DNA damage with the Comet Assay IV software. The tail moment comet parameter (mean ± SD) was used as an indicator of DNA damage [Wu et al., 2011].

Total RNA Isolation

Briefly, following benzidine exposure, cells were washed with cold 1 × PBS. After washing, 1 ml Trizol reagent and 200 μl of chloroform were added. After mixing vigorously, the solution was centrifugated at 13,000*g* for 20 min. The supernatant was isolated, mixed with an equal volume of isopropanol, and incubated for 10 min. This mixture was then centrifuged at 13,000*g* for 10 min. The supernatant was discarded, and the pellet was treated with 70% alcohol and 1 ml of diethylpyrocarbonate (DEPC). After drying, the RNA was dissolved in DEPC. RNA quantity and purity were measured spectrophotometrically (BioPhotometer, Eppendorf). Samples were considered suitable for further processing if the A_{260}/A_{280} ratios were between 1.8 and 2.0. RNA integrity was determined with a 1.8% agarose electrophoresis gel.

Pathway Specific Real-Time PCR Assay

We followed the procedures described by Wu et al. [2011], which used the human DNA damage signaling RT^2 profile PCR array (SuperArray Bioscience) to determine the role of XPC in repairing zidovudine-induced DNA damage in HepG2 cells. Similarly, this array was used to assess the effect of 200 μM benzidine on the expression of 84 genes related to DNA damage responses. Synthesis of complementary DNA, real-time PCR, and statistical analyses was performed according to the manufacturer's instructions. The data shown represent the average of three replicates. Cycle thresholds (C_t) with no more than 35 cycles were determined for each gene product. Five housekeeping genes were included as RNA content controls. Among these five genes, the three (*Rpl13a, B2m*, and *Gapdh*) with the lowest standard derivation across replicates were used for the analysis. The C_t value of each target gene was compared to the average C_t value of these three housekeeping genes. In addition, a genomic DNA control primer set was included in each PCR run to detect the possible DNA contamination. Gene expression differences in the PCR expression array were determined using the $-2\Delta\Delta C_t$ method. Independent experiments were performed in duplicate and repeated at least three times. Statistical significance between treated groups and controls was determined by two-tailed Student's t-test, and $P < 0.05$ was considered significant.

Real-Time Reverse Transcription PCR

To synthesize cDNA from each RNA sample, total RNA (5 μg) was reverse transcribed using MMLV reverse transcriptase (Promega). The resulting samples were diluted 40 times in DNase-free water. Each cDNA solution was stored at −20°C before real-time PCR analysis. Specific oligonucleotide primer pairs were selected from the Roche Univer-

sal Probe Library for the real-time PCR assays. The specificity of each primer pair was validated by performing a RT-PCR reaction using common reference RNA (Stratagene, USA) as a DNA template. The size of the PCR product was verified using a DNA 1000 chip (Agilent Technologies, USA) run on an Agilent Bioanalyzer 2100 (Agilent Technologies, USA). Only primer pairs that generated the predicted product size were chosen to conduct the real-time RT-PCR reactions. RT-PCR reactions were performed on a Roche LightCycler Instrument 1.5 using a LightCycler® FastStart DNA Master^{PLUS} SYBR Green I kit (Roche, Castle Hill, Australia). Briefly, the 10 μl reaction mixtures were composed of 2 μl Master Mix, 2 μl of 0.75 μM forward and reverse primers (a pair of primers for each target gene shown in Table I), and 6 μl cDNA sample. Each sample was run in triplicate. The RT-PCR program consisted of an initial denaturation step at 95°C for 10 min, followed by 40 cycles of amplification and quantification at 95°C for 10 s, 60°C for 15 s, and 72°C for 10 s. At the end of the program, a melt curve analysis was performed. At the end of each RT-PCR run, data were subjected to automated analysis, and an amplification plot was generated for each cDNA sample. From each of these plots, the LightCycler3 Data analysis software automatically calculated the crossing point value, a measure of the beginning of exponential amplification.

Western Blot

Protein extracts (30 μg) were resolved in a 12.5% sodium dodecyl sulfate–polyacrylamide gel, transferred to a PVDF membrane, and blocked with 5% low fat milk at room temperature for 1 hr. After being removed from the low fat milk, the membranes were incubated for 1.5 hr at room temperature with polyclonal mouse anti-PCNA (1:2,000, Santa Cruz, Santa Cruz, CA), anti-β-actin (1:5,000, Santa Cruz), and anti-MUYTH (1:1,000, Abcam, MA). Polyclonal rabbit anti-ERCC1 (1:2,500, Epitomics, Burlingame, USA) and polyclonal goat antipolyclonal p53 (1:1,000, Abcam) were also used. The membranes were then washed three times with 1 × TBS-T buffer (pH = 7.4). Subsequently, the membranes were incubated with horseradish peroxidase-conjugated anti-rabbit, anti-goat, or anti-mouse antibodies (1:5,000, Santa Cruz) for 1 hr at room temperature and washed three times as described earlier. Bands were detected after the addition of chemiluminescent HRP (Immunobilon Western, Millpore). The band density was measured with ImageQuant-TL7.0 software (GE Healthcare).

Detection of Apoptotic Cells

Annexin V/PI staining was performed according to the manufacturer's protocol (BD Biosciences). After treatment for 24 hr with 0, 50, 100, 200, or 400 μM benzidine, cells were washed with cold PBS and resuspended in binding buffer (10 mM HEPES, pH 7.4, 140 mM NaCl, 2.5 mM $CaCl_2$). The cells were then transferred to a mixture containing 5 μl of annex-V-FITC and 10 μl of PI (50 μg/ml) and incubated at room temperature in the dark for 15 min. Binding buffer (400 μl) was then added, and cells were analyzed with flow cytometry (Cell Lab Quanta^{TM} SC, Beckman).

Analysis of Cell-Cycle Progression

The cells (1×10^6/ml) were treated with benzidine (0–200 μM) for 24 hr. At the end of the incubation period, cells were washed with cold PBS (4°C), harvested, and fixed in 70% ethanol at −20°C overnight. The supernatant was then removed, and the cellular pellet was added to a propidium iodine mixture (0.1% Triton X-100, 0.2 mg/ml RNase A, and 20 μg/ml propidium iodine) for 30 min at 37°C. Fluorescence was measured using flow cytometry (Cell Lab Quanta SC).

TABLE I. A Primers Used for Quantitative Real-Time PCR

Gene	Primer sequences
Ercc1	Forward 5′-CATCATTGTGAGCCCTCG-3′
	Reverse 5′-TAGTCTGGGTGCAGGTT-3′
Exo1	Forward 5′-TAGATTGCCTCGTGGCTC-3′
	Reverse 5′-AGTCCATTTCCAAACTGGT-3′
Fen1	Forward 5′-TCTGAGGAGCGAATCCG-3′
	Reverse 5′-CAGTCTTTGCCTTCTTCTTAGT-3′
Mutyh	Forward 5′-CACCTTCTCTCACATCAAGC-3′
	Reverse 5′-GCCCTGATACACACGGA-3′
Mrella	Forward 5′-CAGAACAGATGGCTAATGACTC-3′
	Reverse 5′-ATTCTTAGTAGTGACATTTCGGG-3′
Pcna	Forward 5′-TCCATCCTCAAGAAGGTGTT-3′
	Reverse 5′-GGTAGGTGTCGAAGCCC-3′
B2m	Forward 5′-TGGCCTTAGCTGTGCTC-3′
	Reverse 5′-TGTCGGATGGATGAAACCC-3′
Rpl13a	Forward 5′-AAGGTGTTTGACGGCAT-3′
	Reverse 5′-CTCTTCTCCTCCAGGGT-3′

Data Analysis

For the Comet assay, images of 300 randomly selected cells per sample (three slides/experiment and 100 random cells/slide) were analyzed and divided by three, such that the scoring unit was based on 100 random cells. The mean tail moment from three slides in each experiment was obtained. The difference between the mean tail moments of the control and test groups from the three independent experiments was analyzed using a one-way analysis of variance (ANOVA), where the level of DNA damage was the dependant variable, and benzidine concentration was the independent variable. If a significant F-value was obtained, a Dunnett's multiple comparison test was conducted. Significance was defined as $P < 0.05$.

The DAVID2008 online platform (http://david.abcc.ncifcrf.gov/gene2gene.jsp) was used to conduct a functional enrichment analysis of significantly altered genes [Huang et al., 2009]. Significance was defined as $P < 0.05$.

RESULTS

Benzidine Induces DNA Damage in HepG2 Cells

The viability of HepG2 cells treated with benzidine (25–400 μM) for 24 hr was evaluated. Results showed >90% viability at benzidine concentrations below 200 μM (Fig. 1). To detect genotoxicity, benzidine concentrations below 200 μM were used for the Comet assay. In the Comet assay, the level of DNA damage was evaluated by calculating the tail moment with the aid of the Comet Assay IV software (Fig. 2). DNA damage was increased in a dose-dependent manner (Fig. 2). Positive control (cells treated with 100 μM H_2O_2) and a negative control (cells treated with 0.5% DMSO, a solvent for benzidine) groups were included in the Comet assay, showing tail moments of 15 and 2 unit length, respectively.

Benzidine Induces DNA Damage Responsive Genes

It has been shown that a 24-hr exposure results in more gene expression changes than shorter treatments [Dandrea

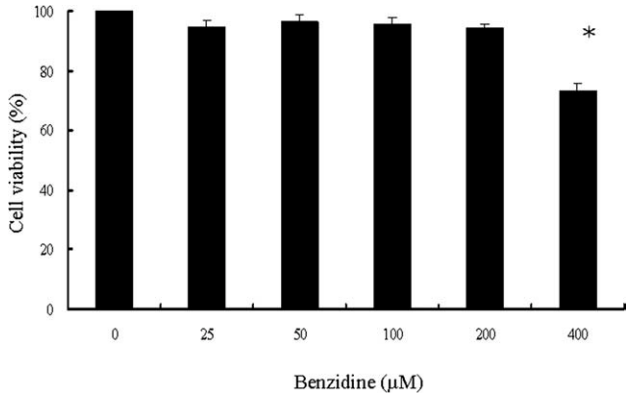

Fig. 1. Cell viability of HepG2 cells exposed to different doses of benzidine for 24 hr. Values represent the mean ± SD and are derived from at least three independent experiments. Triplicate measurements were performed for each experiment. *$P < 0.05$ (vs. control cells).

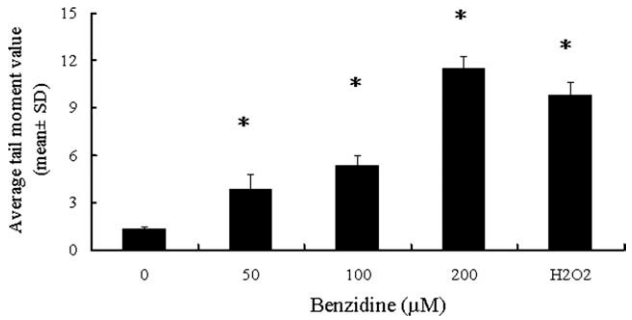

Fig. 2. DNA damage determined by the Comet assay in HepG2 cells treated with benzidine for 24 hr. About 100 μM H_2O_2 was used as a positive control. Values represent the mean ± SD from at least three independent experiments. Triplicate measurements were performed for each experiment. *$P < 0.05$ (vs. control cells).

et al., 2004]. The treatment length selected for the present study is the most frequently found in previously published in vitro gene expression studies and thus provides a suitable time point for comparison across studies [Arbillaga et al., 2007]. A pathway-based PCR expression array (SuperArray Bioscience) was used to determine the expression profile of 84 genes involved with DNA damage signaling following an exposure to 200 μM of benzidine for 24 hr. Results revealed that 23 genes were upregulated by twofold or more ($P < 0.05$), and 1 gene was downregulated ($P < 0.05$) (Table II) when compared with those corresponding genes in the untreated control. The upregulated genes were involved in damage sensing (*Mre11a, Fancg, Rad9a*, and *Rad18*), double-strand break repair (DBR; *Brca1, Rad51, Pcna, Xrcc2*, and *Xrcc3*), base excision repair (*Mutyh, Fen1*, and *Lig1*), nucleotide excision repair (NER; *Ercc1*), mismatch repair (MMR; *Exo1, Trex1*, and *Mlh3*), cell-cycle arrest (*Btg2, Chek1, Gtse1, Mapk12*, and *Sens1*), and apoptosis (*Cidea, Tp73*, and *Ip6k3*). Only *Mlh3* was downregulated (Table II). Of 13 different DNA repair genes, five randomly selected genes (*Ercc1, Exo1, Fen1, Mutyh*, and *Pcna*) belonging to different DNA repair pathways were further confirmed with quantitative real-time PCR (Fig. 3). We found that the expression of these genes was significantly increased when the cells were treated with increasing concentrations of benzidine (0, 100, and 200 μM; Fig. 3).

TABLE II. Gene Expression in 200 μM Benzidine-Treated Cells versus Control Cells for 24 hr

Functional group[a]	Gene	Reference sequence	Fold change	*P* value
Damage sensors	*Mre11a*	NM_005590	2.98 ± 0.13	0.020
	Fancg	NM_004629	3.89 ± 0.16	0.017
	Rad9a	NM_004584	2.57 ± 0.11	0.023
	Rad18	NM_020165	2.31 ± 0.10	0.026
Double-strand break repair	*Brca1*	NM_007294	4.41 ± 0.19	0.016
	Rad51	NM_002875	3.58 ± 0.15	0.018
	Pcna	NM_182649	2.86 ± 0.12	0.021
	Xrcc2	NM_005431	3.06 ± 0.13	0.020
	Xrcc3	NM_005432	3.53 ± 0.15	0.018
Base-excision repair	*Mutyh*	NM_012222	2.20 ± 0.09	0.028
	Fen1	NM_004111	4.15 ± 0.18	0.016
	Lig1	NM_000234	4.62 ± 0.20	0.015
Nucleotide excision repair	*Ercc1*	NM_001983	2.18 ± 0.09	0.028
Mismatch repair	*Exo1*	NM_130398	3.89 ± 0.16	0.017
	Trex1	NM_016381	2.37 ± 0.10	0.025
Cell-cycle arrest	*Btg2*	NM_006763	4.35 ± 0.18	0.016
	Chek11	NM_001274	3.01 ± 0.13	0.020
	Gtse1	NM_016426	2.96 ± 0.12	0.021
	Mapk12	NM_002969	2.98 ± 0.13	0.020
	Sesn1	NM_014454	2.51 ± 0.11	0.024
Apoptosis	*Cidea*	NM_001279	2.07 ± 0.09	0.030
	Tp73	NM_005427	5.45 ± 0.23	0.014
	Ip6k3	NM_054111	5.96 ± 0.25	0.014
Mismatch repair	*Mlh3*	NM_014381	−7.21 ± 0.30	0.010

[a]The functional groups were categorized using the human DNA damage signaling RT^2 profile PCR array manual (SuperArray Bioscience).

Detection of Apoptosis and Cell-Cycle Arrest

Flow cytometry was used to determine cell-cycle progression and apoptosis following a 24-hr exposure to 0, 50, 100, 200, or 400 μM benzidine. As shown in Figure 4, the percentage of the cell population in the G2/M phase was 21.6, 40.4, 39.8, 46.6, or 45.8% for cells treated with 0, 50, 100, 200, or 400 μM benzidine, respectively. These findings indicate that G2/M arrest occurred after exposure to benzidine. To evaluate the possibility of benzidine-induced apoptosis, cells were stained with PI and annexin V. In the absence of benzidine, minimal numbers of apoptotic cells were observed (Fig. 5a). PI is used to identify cells in the early stages of apoptosis, whereas annexin V stains late stage apoptotic cells. The sum ratio of early and late apoptotic cells was increased in benzidine-treated cells (Fig. 5f; $P < 0.05$).

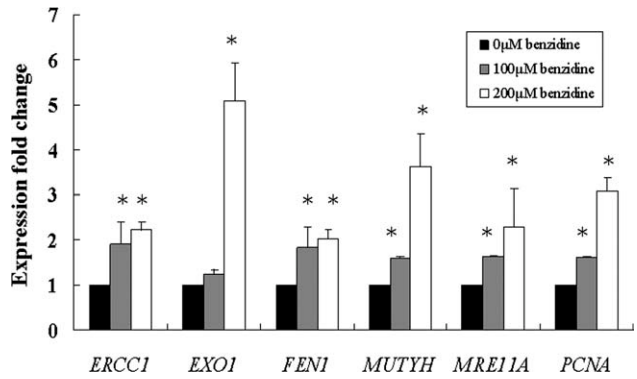

Fig. 3. Gene expression changes in HepG2 cells exposed to benzidine for 24 hr using quantitative real-time PCR. Values represent the mean ± SD of at least three independent experiments. *$P < 0.05$ (vs. control cells).

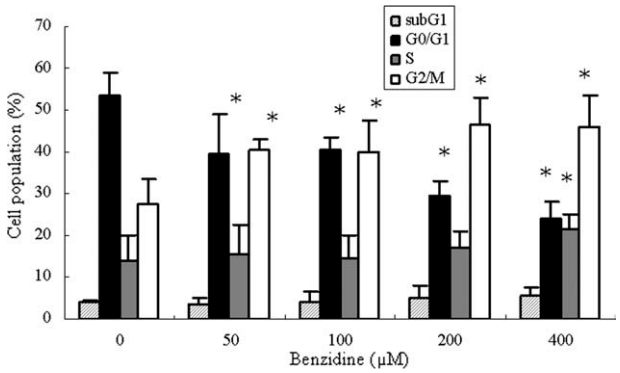

Fig. 4. Effect of a 24-hr exposure to benzidine on cell-cycle distribution in HepG2 cells using flow cytometry. Values represent the mean of three independent experiments.

The Induction of DNA Repair Proteins

Changes observed at the transcription level for *Ercc1*, *Pcna*, and *Mutyh* were confirmed at the protein level with Western blot analysis (Figs. 6a–6d). Western blots confirmed the changes in gene expression and revealed a dose-dependent increase in expression of ERCC1, PCNA, and MUTYH proteins in benzidine-treated cells. Increases in p53 proteins were also observed in HepG2 cells after treatment with benzidine (0–400 μM) for 24 hr (Fig. 6d).

DISCUSSION

HepG2 cells derived from a human hepatoma were chosen as the model for this study because of their human origin and retention of xenobiotic-metabolizing enzyme activity. These characteristics make them a better model of intact liver than other in vitro systems [Hu et al., 2004]. Additionally, these cells possess certain enzymes that metabolize genotoxic carcinogens [Uhl et al., 1999] and have been used to detect carcinogens, including aflatoxins, heterocyclic aromatic amines, polycyclic aromatic hydrocarbons, and pyrrolidine alkaloids [Knasmuller et al., 1998]. The Comet assay was used to detect the genotoxicity of benzidine in HepG2 cells. We found that, at concentrations of 50–200 μM, benzidine caused an increase in DNA damage.

Gene expression analysis is a useful tool to elucidate mechanisms of genotoxicity and distinguish DNA reactive and DNA nonreactive genotoxins in vitro [Arbillaga et al., 2007]. Previous studies have shown that 24-hr exposures result in more gene expression changes than shorter time treatments [Dandrea et al., 2004], and this treatment time is more frequently found in previously published in vitro gene expression studies [Arbillaga et al., 2007]. At 200 μM, benzidine caused slight cytotoxicity and maximal genotoxicity in HepG2 cells. After a 24-hr exposure to 200μM benzidine, cells were analyzed for changes in the expression of genes involved in cell-cycle arrest, apoptosis, and DNA repair.

Upregulation of five cell-cycle-related genes (*Mapk12*, *Gtse1*, *Chek1*, *Btg2*, and *Sens1*) was observed in benzidine-treated cells. MAPK12, also known as p38gamma, is required for gamma irradiation-induced G2 arrest [Wang et al., 2000]. GTSE-1 regulates p21(CIP1/WAF1) stability, conferring resistance to paclitaxel. Precise regulation of p21(CIP1/WAF1) levels is critical for cell-cycle control and cellular responses to stress [Bublik et al., 2010]. CHEK1 (CHK1) activity was previously found to be important for G2 arrest following DNA damage [Jackson et al., 2000]. Btg2 participates in cell-cycle arrest and p53 signaling [Mollerstrom et al., 2010]. SESN1 (PA26) is a novel target of p53 tumor suppressor and growth arrest inducible genes [Velasco-Miguel et al., 1999]. We confirmed induction of G2 phase arrest in a dose-dependent manner (Fig. 4), thus induction of cell-cycle control genes is consistent with the observed molecular changes.

Apoptosis is a cellular defense mechanism [Davies, 2000]. The apoptosis-related genes, *Cidea*, *Tp73*, and *Ip6k3*, were upregulated. CIDE-A activates apoptosis in mammalian cells [Inohara et al., 1998], and redistribution of CIDE-A from mitochondria to the nucleus is associated with apoptosis in HeLa cells treated with tetracycline [Valouskova et al., 2008]. TP73 is a member of the TP53 tumor suppressor gene family that is overexpressed in a variety of tumors and mediates apoptotic responses to genotoxic stress [Castellino et al., 2007]. At the protein level, our data confirmed the induction of apoptosis following benzidine treatment (Fig. 5). However, cells with DNA damage that escape apoptosis may eventually undergo malignant transformation [Kumari et al., 2009].

The DNA damage-related genes, *Rad9a*, *Rad18*, *Fancg*, and *Mre11a*, were upregulated. RAD9A is required for the Claspin protein to bind to sites of DNA damage, facil-

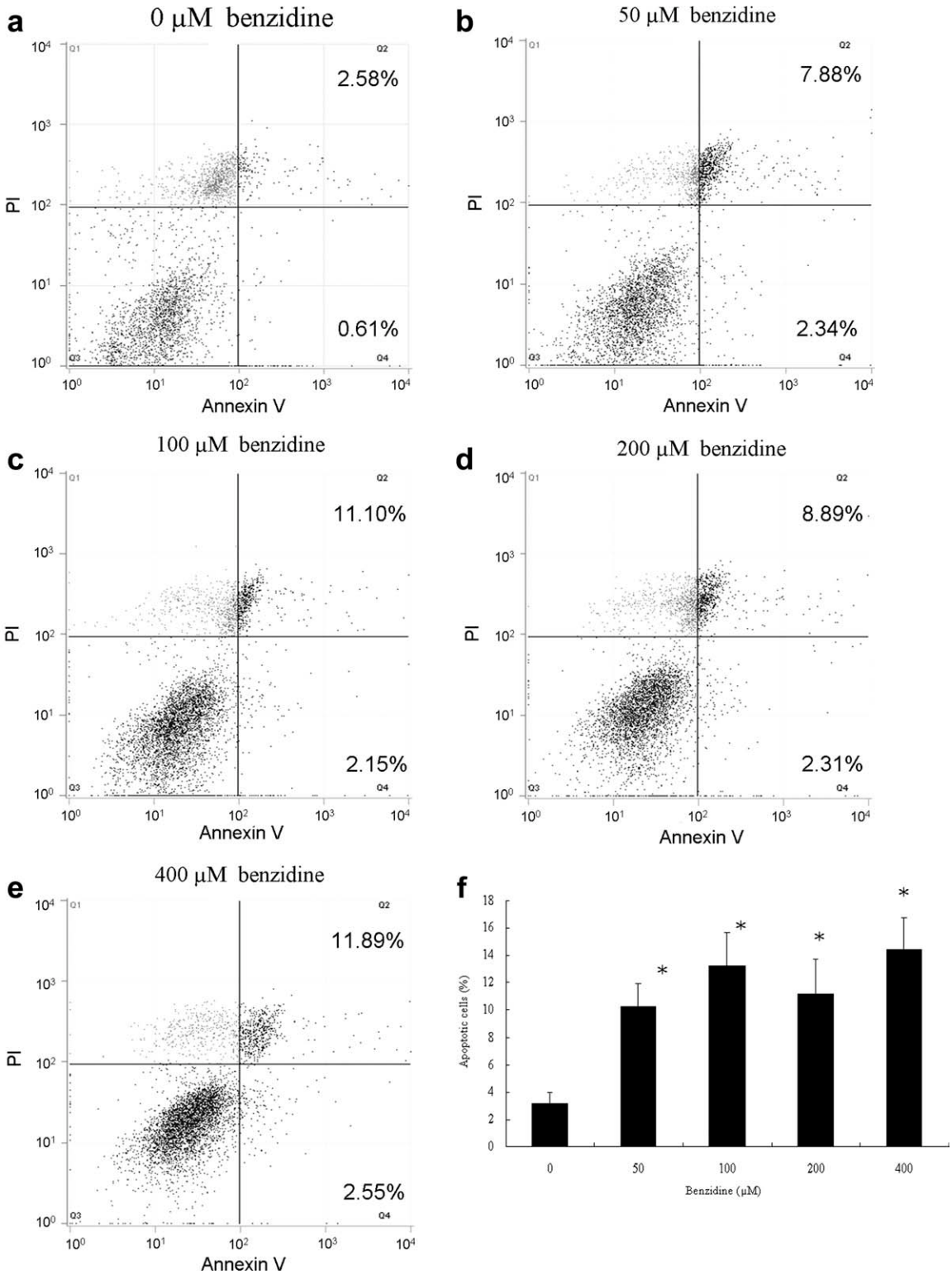

Fig. 5. Effect of benzidine on apoptosis in HepG2 cells using flow cytometry with annexin V and PI staining. (**a**) 0 μM benzidine, (**b**) 50 μM benzidine, (**c**) 100 μM benzidine, (**d**) 200 μM benzidine, (**e**) 400 μM benzidine, and (**f**) $^*P < 0.05$ (vs. control cells). Values are derived from at least three independent experiments.

itating its role during CHK1-mediated checkpoint responses [Sierant et al., 2010]. The FANCG protein exists as a monomer under nonoxidizing conditions, but forms a polymer following H_2O_2 treatment. This protein uniquely responds to oxidative damage by forming complexes via intermolecular disulfide linkages [Park et al.,

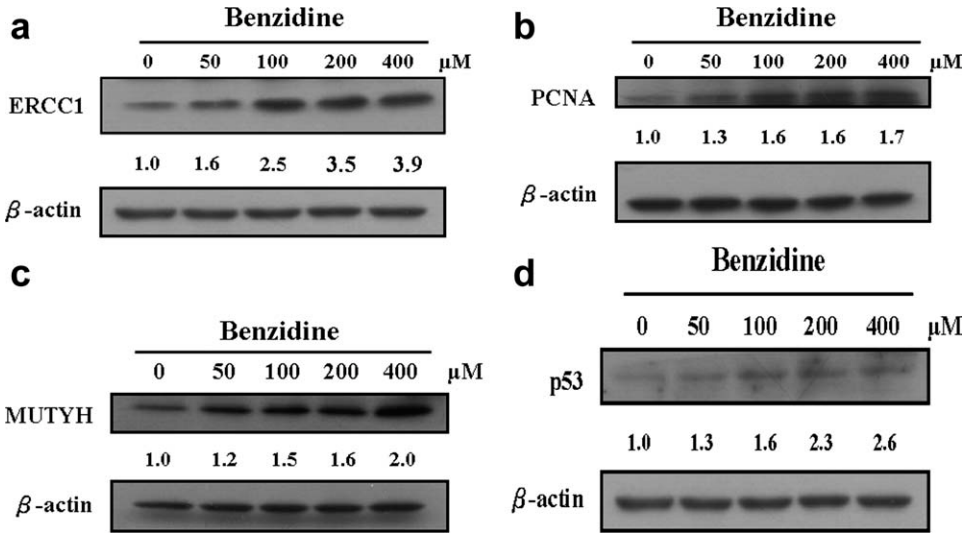

Fig. 6. Western blot analysis of (**a**) ERCC1, (**b**) PCNA, (**c**) MUTYH, and (**d**) p53 protein expression in HepG2 cells treated with benzidine for 24 hr. Values represent the fold change of the protein expression in benzidine-treated cells compared to controls. Values are derived from at least three independent experiments.

2004]. RAD18-mediated translesion synthesis of bulky DNA adducts is coupled to activation of the Fanconi anemia DNA repair pathway [Song et al., 2010]. Oxidative stress induces cell-cycle-dependent MRE11 recruitment, ATM and CHK2 activation, and histone H2AX phosphorylation [Zhao et al., 2008].

The changes in DNA repair genes were largest among genes involved in DNA damage signaling pathways (Table II). These DNA repair genes were involved in four different DNA repair pathways, including DBR, base-excision repair (BER), NER, and MMR. Only one gene, *Mlh3*, functioning in the MMR pathway was downregulated. The downregulation of some DNA repair genes, including *Mlh3*, is associated with pathogenesis and poor prognosis of astrocytomas [Jiang et al., 2006]. However, the role of *Mlh3* in benzidine-induced DNA damage is still unknown. Ontology/pathway analysis using The Database for Annotation, Visualization and Integrated Discovery (DAVID) [Huang et al., 2009] revealed that both DBR and MMR are major DNA repair pathways that respond following benzidine treatment (Table III). Thus, five DNA repair genes (*Pcna*, *Mutyh*, *Ercc1*, *Exo1*, and *Fen1*) were selected from each pathway for confirmation using real-time PCR and western blotting (Figs. 3 and 6). Each of these genes was confirmed to respond to benzidine using these alternative methods. PCNA is involved in DNA repair induced by alkylating agents or oxidative damage in human fibroblasts [Savio et al., 1998]. MUTYH and FEN1 proteins repair lesions produced by 7,8-dihydro-8-oxoguanine (8-oxo-G), a highly mutagenic lesion that causes genomic instability and contributes to carcinogenesis [van Loon et al., 2009]. ERCC1 is a specific target for oxidative stress-induced modification of NER [Langie et al., 2007]. Although NER mainly repairs bulky DNA adducts and helix distorting lesions, it can also act as a backup system for BER in removing oxidative DNA damage [Langie et al., 2007]. EXO1 is implicated in the repair of DNA mismatches [Schmutte et al., 2001]. In addition to these DNA repair proteins, the P53 protein is also associated with DNA repair [Xu et al., 1993]. The P53 pathway has been shown to mediate cellular stress responses and can initiate DNA repair [Vazquez et al., 2008]. A loss in expression of genes involved in DNA repair pathways might result in oncogenesis.

TABLE III. Functional Annotation Analysis of Differentially Expressed Genes Using DAVID [Huang et al., 2009]

Signaling pathways	200 μM benzidine (*P* value)
Apoptosis	3.1E-2
Regulation of cell cycle	1.8E-3
Double-strand break repair	4.3E-8
Mismatch repair	3.6E-10
Damaged DNA binding	1.0E-8

A pathway was considered affected when at least two genes within the pathway were significantly modulated by benzidine treatment. Pathways were considered significant at a *P*-value below 0.05.

In summary, after a 24-hr exposure to benzidine, we observed upregulation of 23 genes involved in apoptosis, DNA repair, and cell-cycle arrest in HepG2 cells. The upregulation of these genes was consistent with the DNA damage response, alterations in cell cycle, and induction of apoptosis observed in the cells. Overexpression of these genes suggests that benzidine operates through a DNA reactive genotoxic mechanism.

REFERENCES

Arbillaga L, Azqueta A, van Delfet JHM, de Cerain AL. 2007. In vitro gene expression data supporting a DNA non-reactive genotoxic mechanism for orchratoxin A. Toxicol Appl Pharmacol 220: 216–224.

Bublik DR, Scolz M, Triolo G., Monte M, Schneider C. 2010. Human GTSE-1 regulates p21(CIP1/WAF1) stability conferring resistance to paclitaxel treatment. J Biol Chem 285:5274–5281.

Castellino RC, de Bortoli M, Lin LL, Skapura DG, Rajan JA, Adesina AM, Perlaky L, Irwin MS, Kim JY. 2007. Overexpressed TP73 induces apoptosis in medulloblastoma. BMC Cancer 7:127.

Chen SC, Kao CM, Huang MH, Shih MK, Chen YL, Huang SP, Liu TZ. 2003. Assessment of genotoxicity of benzidine and its structural analogues to human lymphocytes using Comet assay. Toxicol Sci 72:283–288.

Chen SC, Lin CS, Liang SH, Chung JY. 2006. Detection of genotoxicity of benzidine and its derivatives with *Escherichia coli* DJ 702 LacZ reversion mutagenicity assay. Lett Appl Microbiol 43: 22–26.

Chung KT, Cerniglia CE. 1992. Mutagenicity of azo dyes: Structure-activity relationships. Mutat Res 2:267–269.

Chung KT, Chen SC, Wong TY, Wei CI. 1998. Effect of benzidine and benzidine analogues on growth of bacteria including *Azotobacter vinelandii*. Environ Toxicol Chem 2:2121–2132.

Chung KT, Chen SC, Wong TY, Li YS, Wei CI, Chou MW. 2000. Mutagenicity studies of benzidine and its analogues: Structure-activity relationships. Toxicol Sci 56:351–356.

Dandrea T, Hellmold H, Jonsson C, Zhivotovsky B, Hofer T, Wärngård L, Cotgreave I. 2004. The transcriptional response of human A549 lung cells to a hydrogen peroxide-generating system: Relationship to DNA damage, cell cycle arrest, and caspase activation. Free Radic Biol Med 36:881–896.

Davies KJA. 2000. Oxidative stress, antioxidant defenses, and damage removal, repair and replacement systems. IUBMB Life 50: 279–289.

Grady MK, Jacobson-Kram D, Dearfield KL, Williams JR. 1986. Induction of sister chromatid exchanges by benzidine in rat and human hepatoma cell lines and inhibition by indomethacin. Cell Biol Toxicol 2:223–230.

Hu T, Gibson DP, Carr GJ, Torontali SM, Tiesman JP, Chaney JG, Aardema MJ. 2004. Identification of a gene expression profile that discriminates indirect-acting genotoxins and direct-acting genotoxins. Mutat Res 549:5–27.

Huang DW, Sherman BT, Lempicki RA. 2009. Systematic and integrative analysis of large gene lists using DAVID bioinformatics resources. Nat Protoc 4:44–57.

Inohara N, Koseki T, Chen S, Wu X, Nunez G. 1998. CIDE, a novel of cell death activator with homology to the 45 kDa subunit of the DNA fragmentation factor. EMBO J 17:2526–2533.

Jackson JR, Gilmartin A, Imburgia C, Winkler JD, Marshall LA, Roshak A. 2000. An indolocarbazole inhibitor of human checkpoint kinase (Chk1) abrogates cell cycle arrest caused by DNA damage. Cancer Res 60:566–572.

Jiang Z, Hu J, Li X, Jiang Y, Zhou W, Lu D. 2006. Expression analysis of 27 DNA repair genes in astrocytoma by Taqman low-density array. Neurosci Lett 1409:112–117.

Knasmuller S, Parzefall W, Sanyal R, Ecker S, Schwab C, Uhl M, Mersch-Sundermann V, Williamson G, Hietsch G, Langer T, Darroudi F, Natarajan AT. 1998. Use of metabolically competent human hepatoma cells for the detection of mutagens and antimutagens. Mutat Res 402:185–202.

Kumari R, Singh KP, DuMond JW Jr. 2009. Simulated microgravity decreases DNA repair capacity and induces DNA damage in human lymphocytes. J Cell Biochem 107:723–731.

Langie SA, Knaapen AM, Houben JM, van Kempen FC, de Hoon JP, Gottschalk RW, Godschalk RW, van Schooten FJ. 2007. The role of glutathione in the regulation of nucleotide excision repair during oxidative stress. Toxicol Lett 168: 302–309.

Makena PS, Chung KT. 2007a. Effects of various polyphenols on bladder carcinogen benzidine-induced mutagenicity. Food Chem Toxicol 45:1899–1909.

Makena PS, Chung KT. 2007b. Evidence that 4-aminobiphenyl, benzidine, and benzidine congeners produce genotoxicity through reactive oxygen species. Environ Mol Mutag 48: 404–413.

Mollerstrom E, Kovac A, Lovgren K, Nemes S, Delle U, Danielsson A, Parris T, Brennan DJ, Jirström K, Karlsson P, Helou K. 2010. Up-regulation of cell cycle arrest protein BTG2 correlates with increased overall survival in breast cancer, as detected by immunohistochemistry using tissue microarray. BMC Cancer 10:296.

Morikawa Y, Shiomi K, Ishihara Y, Matsuura N. 1997. Triple primary cancers involving kidney, urinary bladder, and liver in a dye worker. Am J Ind Med 31:44–49.

Park SJ, Ciccone SL, Beck BD, Hwang B, Freie B, Clapp DW, Lee SH. 2004. Oxidative stress/damage induces multimerization and interaction of Fanconi anemia proteins. J Biol Chem 279: 30053–30059.

Savio M, Stivala LA, Bianchi L, Vannini V, Prosperi E. 1998. Involvement of the proliferating cell nuclear antigen (PCNA) in DNA repair induced by alkylating agents and oxidative damage in human fibroblast. Carcinogenesis 19:591–596.

Schmutte C, Sadoff MM, Shim KS, Acharya S, Fishel R. 2001. The interaction of DNA mismatch repair proteins with human exonuclease I. J Biol Chem 276:33011–33018.

Sierant ML, Archer NE, Davey SK. 2010. The Rad9A checkpoint protein is required for nuclear localization of the claspin adaptor protein. Cell Cycle 9:548–556.

Song IY, Palle K, Gurkar A, Tateishi S, Kupfer GM, Vaziri C. 2010. Rad18 mediated translesion synthesis of bulky DNA adducts is coupled to activation of the Fanconi anemia DNA repair pathway. J Biol Chem 285:31525–31536.

Uhl M, Helma C, Knasmuller S. 1999. Single cell gel electrophoresis assays with human-derived hepatoma (HepG2) cells. Mutat Res 441:215–224.

Valouskova E, Smolkova K, Santorova J, Jezek P, Modriansky M. 2008. Redistribution of cell death-inducing DNA fragmentation factor-like effector-a (CIDEa) from mitochondria to nucleus is associated with apoptosis in HeLa cells. Gen Physiol Biophys 17:92–100.

van Loon B, Hubscher U. 2009. An 8-oxo-guanine repair pathway coordinated by MUTYH glycosylase and DNA polymerase lambda. Proc Natl Acad Sci USA 106:18201–18206.

Vazquez A, Bond EE, Levine AJ, Bond GL. 2008. The genetic of the p53 pathway, apoptosis and cancer therapy. Nat Rev Drug Discov 12:979–987.

Velasco-Miguel S, Buckbinder L, Jean P, Gelbert L, Talbott R, Laidlaw J, Seizinger B, Kley N. 1999. PA26, a novel target of the p53 tumor suppressor and member of the GADD family of DNA damage and growth arrest inducible genes. Oncogene 18: 127–137.

Wang X, McGowan CH, Zhao HeL, Downey JS, Fearns C, Wang Y, Huang S, Han J. 2000. Involvement of the MKK6-p38γ cascade in gamma-radiation-induced cell cycle arrest. Mol Cell Biol 20:4543–4552.

Wang SC, Chung JG, Chen CH, Chen SC. 2006. 2-and 4-Aminobiphenyl induce oxidative DNA damage in human hepatoma (HepG2) cells via different mechanisms. Mutat Res 593:9–21.

Wu JC, Hseu YC, Chen CH, Wang SH, Chen SC. 2009. Comparative investigations of genotoxic activity of five nitriles in the Comet assay and the Ames test. J Hazard Mater 169: 492–497.

Wu Q, Beland FA, Chung CW, Fang JL. 2011. XPC is essential for nucleotide excision repair of zidovudine-induced DNA damage in human hepatoma cell. Toxicol Appl Pharmacol 251: 155–162.

Wu JC, Chye SM, Shih MK, Chen CH, Yang HL, Chen SC. Genotoxicity of dicrotophos, an organophosphorous pesticide, assessed with different assay *in vitro*. Environ Toxicol. 2010 Dec 8. [Epub ahead of print].

Xu J, Morris GF. 1993. p53-mediated regulation of proliferating cell nuclear antigen expression in cells exposed to ionizing radiation. Mol Cell Biol 19:12–20.

Zhao H, Traganos F, Albino AP, Darzynkiewicz Z. 2008. Oxidative stress induces cell cycle-dependent Mre11 recruitment ATM, Chk2 activation and histone H2AX phosphorylation. Cell Cycle 7:1490–1495.